Science of the Total Environment 903 (2023) 166560

Contents lists available at ScienceDirect

Science of the Total Environment

journal homepage: www.elsevier.com/locate/scitotenv

New insights into the impact of polystyrene micro/nanoplastics on the nutritional quality of marine jacopever (*Sebastes schlegelii*)

Xuemei Sun [a,b], Xuru Wang [a,c], Andy M. Booth [d,*], Lin Zhu [a,b], Qi Sui [a], Bijuan Chen [a,b], Keming Qu [a], Bin Xia [a,b,**]

[a] State Key Laboratory of Mariculture Biobreeding and Sustainable Goods, Yellow Sea Fisheries Research Institute, Chinese Academy of Fishery Sciences, Qingdao 266071, China
[b] Laboratory for Marine Ecology and Environmental Science, Laoshan Laboratory, Qingdao 266237, China
[c] College of Marine Sciences, Shanghai Ocean University, Shanghai 201306, China
[d] SINTEF Ocean, Department of Climate and Environment, Trondheim 7465, Norway

HIGHLIGHTS

- Toxicity indicators of fish affected by PS-NPs are greater than those by PS-MPs.
- Endocytosis of MPs and NPs induce different fish nutritional reduction.
- NPs triggered more cell apoptosis in Ferroptosis and FoxO signaling pathways than MPs.
- Mitochondria are the major cellular targets of PS MPs/NPs for marine fish.
- NPs introduced higher genes expression related to electron transfer chain than MPs.

GRAPHICAL ABSTRACT

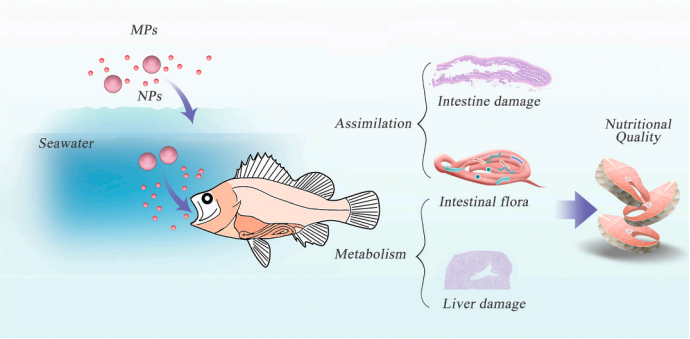

ARTICLE INFO

Editor: Damia Barcelo

Keywords:
Polystyrene
Microbial community structure
Hepatocyte metabolism
Hepatic transcriptome
Nutritional quality

ABSTRACT

Microplastics (MPs) and nanoplastics (NPs) are ubiquitous in the marine environments due to the wide use and mismanagement of plastics. However, the effect of MPs/NPs on the nutrition quality of economic species is poorly understood, and their underlying mechanisms remained unclear. We therefore investigated the impacts of polystyrene MPs/NPs on the nutrition composition of marine jacopever *Sebastes schlegelii* from the perspective of assimilation and metabolism. Results showed that NPs reduced more nutrition quality than MPs. Despite no notable impact on intestinal microbiota function, MPs/NPs influenced the assimilation of fish through intestinal damage. Furthermore, NPs induced greater damage to hepatocyte metabolism than MPs, caused by hepatocyte uptake through membrane protein pumps/channels and clathrin/caveolin-mediated endocytosis for NPs, while through phagocytosis/pinocytosis for MPs. NPs triggered more cell apoptosis signals in Ferroptosis and FoxO signaling pathways than MPs, destroying mitochondria structure. Compared with MP treatments, a significant upregulation of genes (*PRODH* and *SLC25A25A*) associated with the electron transfer chain of mitochondria was

* Corresponding author.
** Correspondence to: B. Xia, State Key Laboratory of Mariculture Biobreeding and Sustainable Goods, Yellow Sea Fisheries Research Institute, Chinese Academy of Fishery Sciences, Qingdao 266071, China.
E-mail addresses: andy.booth@sintef.no (A.M. Booth), xiabin@ysfri.ac.cn (B. Xia).

https://doi.org/10.1016/j.scitotenv.2023.166560
Received 28 June 2023; Received in revised form 22 August 2023; Accepted 23 August 2023
Available online 24 August 2023

detected in the NP treatments, influencing the tricarboxylic acid cycle and interfering with liver metabolism of proteins, fatty acid, glycerol phospholipids, and carbohydrates. This work provides new insights into the potential impacts of MPs/NPs on the quality and safety of seafood.

1. Introduction

Microplastics (MPs, 1 μm–5 mm) have been shown to be ubiquitous in all compartments across the global marine environments. Despite challenges with extraction and analysis of nanoplastics (NPs, <1 μm), it has been reported that one spherical MP particle (5 mm) can be broken down into 10^{14} NPs (100 nm) for several hundreds of years (Wagner and Reemtsma, 2019). Currently, limited studies reported that the numerical abundance of NPs in marine environments is expected to be much higher than MPs (Davranche et al., 2020; Lenz et al., 2016; Ter Halle et al., 2017). NPs can cross the gut barrier and translocate into secondary tissues, even interacting with proteins, and induce the conformational changes and denaturation of protein, while larger sized MPs may be only physically trapped in the gut (Gopinath et al., 2019; Li et al., 2021a; Magri et al., 2018). After fish (common carp juveniles) exposure to polyethylene plastics particles, multi-biomarkers were changed in exposure groups, and more serious damage induced in exposure groups with the decreasing size of polyethylene plastics particles (nano > micro > macro) compared to the control groups (Hamed et al., 2022). Therefore, NPs may pose a greater risk to marine ecosystems than MPs and further effort should be devoted to understanding the impacts of NP pollution (Jeong et al., 2016; Li et al., 2021b).

Economic fish species are a rich source of protein and nutrients (e.g., human-essential amino acids and omega-3 polyunsaturated fatty acids) for many of the global human population. Previous studies have found that MP exposures led to a reduction of energy reserves and nutrition quality (e.g., protein and lipid contents) of marine fish (Lu et al., 2022; Yin et al., 2018), while the reasons for the reduction were not fully investigated. For NPs, only one study found the dietary exposure to polystyrene (PS) NPs altered the fatty acid composition and texture of muscle in carnivorous marine fish large yellow croaker (Lai et al., 2021). Furthermore, it has been reported that there were significant differences on the effects of nanoparticles on the crude protein of marine fish juvenile turbot between dietary exposure and waterborne exposure (Wang et al., 2016). To date, no study focused on the impact of NPs on the nutritional composition of economically important fish species through waterborne exposure, hampering the risk assessment of NPs on the quality and safety of seafood.

As a critical line of defense against exogenous substances, the intestinal tract is a vital organ for controlling digestion, absorption, and immunity in animals (Magalhaes et al., 2007). Furthermore, the liver of fish plays a key role in lipid and toxicant metabolism (Nguyen et al., 2008). Moreover, intestinal microbiota composition can affect bile acid metabolism, which has been implicated in the regulation of lipid, glucose, and energy metabolism (Duparc et al., 2017). PS-MPs have been reported to trigger lipid metabolic disorders via inducing intestinal microbiota dysbiosis in marine medaka (*Oryzias melastigma*) (Zhang et al., 2021a). Therefore, damage to the intestine and liver induced by MPs/NPs has the potential to induce negative impacts on fish digestion and absorption of lipids and other nutrients, such as proteins, sugars, and so on. In turn, this can influence the nutritional quality of fish. However, the potential toxicity mechanisms of MPs and NPs, including the internalization pathway and apoptotic signals, remain unclear.

Sebastes schlegelii is widely distributed in the coastal waters of Southeast Asian, and they are cultured in many countries for the food supply of humans (Zhang et al., 2021b). In this study, juvenile *S. schlegelii* was chosen because of its high ecological and economic values (Kishimura et al., 2007). Relative to MPs, it is hypothesized that exposure to NPs has a greater impact on the nutritional quality of marine economic fish and that this is driven by (i) NPs disturbing intestinal assimilation and (ii) NPs inducing hepatic metabolism due to higher bioavailability and increased endocytosis. To test this hypothesis, we examined the behaviors of MPs/NPs in filtered seawater, and investigated growth parameters and the nutritional quality of economic marine fish. Through the histochemical and multi-omics analyses, the underlying mechanisms of MP/NP exposure influencing the nutrition quality of marine fish were elucidated for the first time.

2. Materials and methods

2.1. Chemicals and test organisms

Red fluorescent non-functionalized polystyrene microspheres (PS-MPs, 5 μm, 1.06 g/cm^3) and nanospheres (PS-NPs, 100 nm) were purchased from Tianjin Unibead Scientific Co. Ltd. (www.qiuhuan.com, Tianjin, China) as dispersions. The morphology, fluorescence, polymeric composition and the primary size of MPs and NPs were characterized. Detailed information regarding the preparation and characterization of the PS-MP/NP dispersions is provided in the Supporting Information (SI).

Juvenile jacopever (*S. schlegelii*) were obtained from Qingdao Qingyuan Marine Biological Technology Co., Ltd. (http://www.qdfenghuangdao.cn/, China). The fish were cultured in filtered seawater with aeration for 15 days, 720 healthy fish (average weight: 2.55 ± 0.78 g; average length: 54.72 ± 5.36 mm) were randomly selected for use in the experiments. The entire exposure medium was renewed daily, and the detail of the culturing was shown in SI. The approval about use of the fish (*S. schlegelii*) was obtained by the ethic committee of Yellow Sea Fisheries Research Institute (Protocol N.2021028; August 22th, 2021).

2.2. Experimental design

The experimental design is summarized in Fig. S1. *S. schlegelii* (n = 720) were randomly distributed to 9 tanks (80 L), with triplicate tanks for control, PS-MPs and PS-NPs samples, respectively. PS particles were added to each tank to achieve final exposure concentrations of 0.23 mg/L. This was considered to environmentally realistic for MPs (Zhang et al., 2019) and so the same concentration was also used for NPs as such values are not currently available. The deposition behavior and zeta potential of PS-MPs and PS-NPs were shown in the SI. The exposure of *S. schlegelii* was conducted over a period of 15 days.

2.3. Assessment of health status and nutritional quality analysis

After 15 days of exposure to PS-MPs and PS-NPs, growth parameters (Weight gain rate, Specific growth rate and Survival rate), biometric parameters (Condition factor, Hepatosomatic index and Viserosomatic index) and nutritional composition (Crude protein, Crude lipid, Moisture and Ash content) were measured and calculated according to methods described in our previous research (Yin et al., 2018). Fresh brain and liver of 60 fishes from each group were removed and vacuum-freeze dried (Labconco, USA), while the rest of the fish was dried at 105 °C until a constant weight was recorded. Then all the dried fish were grounded together into powder and the changes of water content (Moisture) and body composition matter (Crude protein, Crude lipid and Ash content) were analyzed. Gross energy was measured using an automatic oxygen bomb calorimeter (WZH-15 DJL9, CSCX, China). Crude protein (N × 6.25) was determined by the Kjeldahl method using an auto Kjeldahl System (Buchi B-324/435/412, Switzerland) (2002). Crude lipid was determined by the ether-extraction method (Grisdale-

Helland et al., 2008; Yin et al., 2018). Crude ash was determined by a muffle furnace at 550 °C for 4 h. The detail of calculation was shown in the SI.

2.4. Histopathological and ultrastructural analysis

After exposure to PS-MPs and PS-NPs for 15 days, fresh liver and intestine were extracted from fish ($n = 15$) of each group, and then randomly divided into three samples to be used for the different analyses. The first sample was used for histological analysis, and the detailed information is shown in the SI. The second sample was fixed in glutaraldehyde and embedded in Epon 812 resin (Xia et al., 2020). The 6 μm thick ultrathin sections were prepared using an ultramicrotome (LKB, Sweden) and stained with uranyl acetate and lead citrate. Ultrastructural changes of these samples were then investigated by TEM. The last sample was extracted to analysis of the intestinal microbiota, transcriptomic and metabolomic response of liver.

2.5. DNA extraction and high-throughput sequencing

According to our previous study (Sun et al., 2020a), a detailed description of the library construction process, sequencing and analysis method are provided in the SI. Briefly, the intestine of fish ($n = 15$) each from the control, MP, and NP groups were randomly selected. Due to the young age of the fish, the whole gastrointestinal tract was used. The total DNA in each sample was extracted by the HiPure Soil DNA Kit (Magen, Guangzhou, China), and the amplified products were purified using the AxyPrep DNA Gel Extraction Kit according to the manufacturer's instructions.

2.6. RNA extraction and transcriptome sequencing

For transcriptomic analysis, liver tissues of fish (n = 15) from each groups (the control, PS-MP, and PS-NP groups) were randomly selected across the three experiments for downstream RNA isolation and Quant-Seq analysis. RNA was extracted from frozen liver tissues using a Trizol reagent kit (Invitrogen, Carlsbad, CA, USA), followed by RNA quantification using an Agilent 2100 Bioanalyzer (Agilent Technologies, Palo Alto, CA, USA). The method has been described in our previous study (Zhu et al., 2016), and the details of the library construction, sequencing, analysis method and quantitative real-time PCR assay are provided in the SI. All RNA-Seq data have been submitted to the NCBI SRA database (https://www.ncbi.nlm.nih.gov/sra/PRJNA772565), under accession number PRJNA772565.

2.7. Metabolomic analysis

Hepatic metabolites were respectively extracted from the fish livers ($n = 30$) in the control, MP, and NP groups. Briefly, 50 mg of tissue was homogenized with 500 μL of 4:1 (*v*/v) methanol/water and 600 μL of 2:1 (v/v) chloroform/water. The mixture was centrifuged at 10000*g* for 5 min at 4 °C. The supernatant phase was transferred to a fresh glass vial for analysis. The extracted metabolites were analyzed by liquid chromatography-tandem mass spectrometry (LC-MS/MS) using an ultrahigh pressure (UHP) LC system (Vanquish, ThermoFisher Scientific) fitted with a UPLC BEH Amide column and coupled to Q ExactiveHFX mass spectrometer (Orbitrap MS, Thermo). Raw MS data files were converted to the mzML format using ProteoWizard and then processed by R package XCMS (version 3.2), which included retention time alignment, peak detection and peak matching steps. The processed mass spectrometry data was then subjected to metabolite annotation with an in-house MS2 database (Li et al., 2021b; Zhang et al., 2017).

2.8. Statistical analysis

All experiments were conducted using triplicate samples, except the six duplications of non-target metabolome, and data are expressed as means ± standard deviation (SD). All data were checked for normality and homogeneity of variance before performing statistical comparisons. Differences among groups were identified using VIP ≥ 1 (OPLS-DA model) and *t*-test $p < 0.05$. All statistical analysis was performed using the IBM SPSS 20. Differences were considered significant when $p < 0.05$.

3. Results and discussion

3.1. Characterization of MPs and NPs

TEM, SEM, micro-FTIR and fluorescence microscope analysis confirmed that both MPs and NPs were spherical PS particles with red fluorescence (Fig. 1A–D and S2). The hydrodynamic diameters obtained from dynamic light scattering in the filtered seawater were 143.36 ± 5.11 nm for PS-NPs and 16.94 ± 0.93 μm for PS-MPs at 0 h, respectively (Fig. 1E, F). The hydrodynamic diameter of PS-NPs in seawater was significantly smaller than that of PS-MPs ($p < 0.05$). In deionized water, the repulsion-attraction counteraction can maintain the colloidal stability of NPs (Martinez-Negro et al., 2021). While, the stability of NPs in seawater is strongly influenced by the ionic strength and organic matter in seawater (Booth et al., 2013; Lee and Fang, 2022), where the surface charge of NPs can be gradually neutralized, leading to reduced colloidal stability and aggregation (Booth et al., 2013; Liu et al., 2012). However, this phenomenon is not obvious for MPs.

3.2. Effects of MPs and NPs on growth and nutritional quality

The growth rates (e.g., WGR and SGR) of jacopever in the PS-MPs and PS-NPs groups were significantly reduced compared with the control group ($p < 0.05$) (Table 1), indicating that both PS-MPs and PS-NPs could significantly inhibit the growth of juvenile fish. However, there were no significant differences in growth between the PS-MPs and PS-NPs groups. This is consistent with previous results, where the survival and growth of large yellow croaker also decreased after exposure to PS-NPs (Lai et al., 2021). Furthermore, there were no significant differences in biometric parameters (CF, VSI and HSI) between the control and experiment groups ($p > 0.05$).

Relative to the controls, marine jacopever exposed to PS-NPs exhibited significantly lower gross energy, crude protein, crude lipid and ash content, but higher moisture. Similarly, gross energy, crude protein and crude lipid were decreased after exposure to PS-MPs (15 μm), which is consistent with previous study (Yin et al., 2018). Importantly, significant differences in gross energy, crude lipid and moisture were detected between the PS-MPs and PS-NPs groups, indicating that PS-NPs can cause greater effects on the energy reserve and nutritional quality of marine jacopever than PS-MPs. Although a greater mass of PS-MPs remained in dispersion and interacted with the fish relative to PS-NPs (Fig. 1G), more substantial effects on the nutritional quality of marine jacopever were observed in PS-NPs treatments than PS-MPs. Overall, exposure to PS-MPs and PS-NPs can reduce the growth and nutritional quality of marine fish, potentially leading to decreased production and reduced economic value.

3.3. Histopathological and ultrastructural analysis of intestine and liver

Representative histopathological observations of liver and intestine are shown in Fig. S3, and Fig. S4, respectively. Injury of the top villi, necrosis, exfoliation and partial dissolution of the columnar epithelial cells, and severe vacuolization were detected in the intestinal tissue from both the PS-MPs and PS-NPs exposures (Fig. S4). A similar phenomenon has also been reported in zebrafish after exposure to MPs/NPs (Duan et al., 2022). Damage to the intestinal tract has been proven to reduce the assimilation capacity of nutrients in fish (Awad et al., 2019). Pathological changes, including congested and dilated blood vessels and inflammatory cell infiltration, were also detected in the liver of juvenile

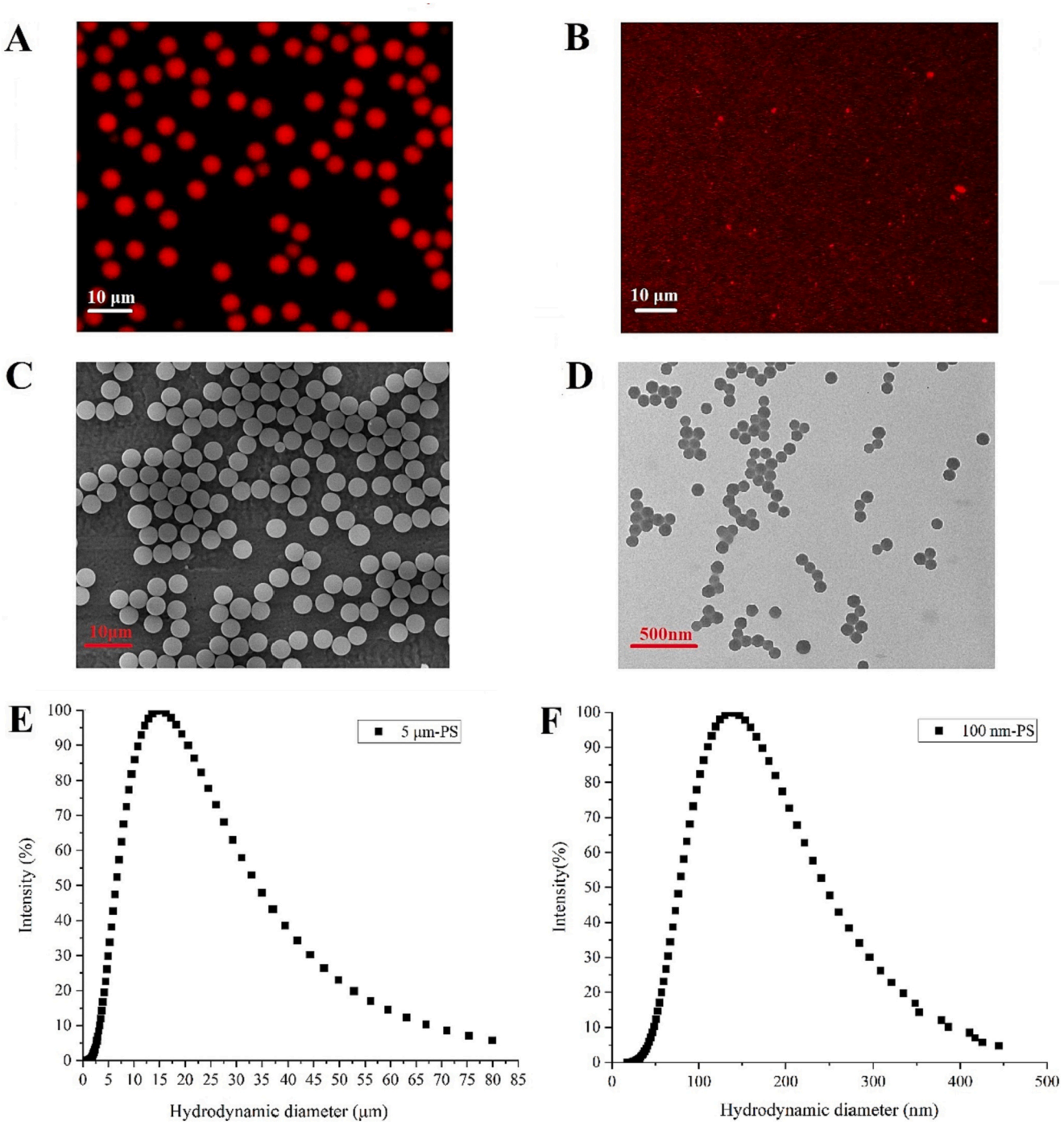

Fig. 1. Characteristics of polystyrene microplastic and nanoplastic test materials. (A) Fluorescence microscopy of PS-MPs. (B) Fluorescence microscopy of PS-NPs. (C) Scanning electron microscopy (SEM) of PS-MPs. (D) Transmission electron microscopy (TEM) of PS-NPs. (E) Hydrodynamic size distribution of commercial PS-MPs in stock solutions at a concentration of 0.23 mg/L in seawater (0 h) determine by dynamic light scattering. (F) Hydrodynamic size distribution of commercial PS-NPs in stock solutions at a concentration of 0.23 mg/L in seawater (0 h) determined by dynamic light scattering.

fish in both PS treatments, especially in the PS-NPs groups (Fig. S3). Interestingly, PS-MPs were observed by fluorescence microscopy in intestine and liver (Fig. S3B and S4B), and PS-NPs were observed by the hyperspectral-enhanced microscopy in intestine and liver (Fig. S5). This also suggests the particles could further enter the circulatory system and then transfer into the hepatocytes (Ma et al., 2022).

The ultrastructures of the intestine and liver were examined using TEM (Fig. 2). In the PS-MPs and PS-NPs groups, a large number of glycogen granules, cytoplasm vacuolation and autophagolysosome were observed in intestinal epithelial cells and hepatocytes, as well as altered mitochondrial morphology (e.g., mitochondrial edema, loss of cristae, and rupturing of the outer mitochondrial membrane) (Fig. 2B and D). Relative to the PS-MPs groups, the PS-NPs groups exhibited more lysosomes, serious disruption of the endoplasmic reticulum and ribosome loss in the epithelial cells of intestine and hepatocytes. Previous studies have also found that the endosomal-lysosomal system and mitochondria were the major target organelles of engineered nanomaterials (Rocha et al., 2015), including NPs (Gaylarde et al., 2021; Sun et al., 2020b; Wu et al., 2021). The PS-NPs induced greater histopathological and ultrastructural damage to intestine and liver of marine jacopever than the PS-

Table 1
Growth performance, biometric parameters, energy and nutritional composition of *S. schlegelii* after exposure to PS-NPs and PS-MPs for 15 days.

Parameters	Control	PS-MPs (5 μm)	PS-NPs (100 nm)
Growth performance (%)			
WGR	11.66 ± 0.99^{a}	7.17 ± 1.39^{b}	6.43 ± 1.98^{b}
SGR	0.73 ± 0.06^{a}	0.46 ± 0.09^{b}	0.41 ± 0.12^{b}
SR	98.67	98.67	98.00
Biometric parameters (%)			
CF	1.43 ± 0.05^{a}	1.48 ± 0.31^{a}	1.52 ± 0.08^{a}
VSI	6.56 ± 1.54^{a}	7.15 ± 1.47^{a}	8.05 ± 1.46^{a}
HSI	1.34 ± 0.68^{a}	1.49 ± 0.41^{a}	2.03 ± 0.64^{a}
Gross energy (KJ/g)	543.84 ± 0.11^{a}	496.03 ± 0.11^{b}	475.63 ± 2.00^{c}
Whole body (%)			
Moisture	65.34 ± 1.14^{a}	68.78 ± 0.65^{a}	70.09 ± 4.90^{b}
Crude protein	19.69 ± 0.65^{a}	17.51 ± 0.37^{b}	16.96 ± 0.68^{b}
Crude lipid	5.62 ± 0.18^{a}	5.34 ± 0.11^{a}	5.05 ± 0.14^{b}
Ash content	3.94 ± 0.23^{a}	3.56 ± 0.15^{ab}	3.52 ± 0.53^{b}

Note: WGR = weight gain rate; SGR = specific growth rate; CF = condition factor; VSI = viserosomatic index; HIS = hepatosomatic index. For a given parameter, different letters (a–c) indicate significant difference among control, PS-NPs and PS-MPs treatments ($n = 6$, $p < 0.05$).

MPs, which may be attributed to the smaller dimensions and colloidal properties of NPs, allowing them to cross cell membrane, and subsequently attack the mitochondria and endoplasmic reticulum to affect cell metabolism.

3.4. Microbiota composition in the intestine

Microbial dysbiosis can cause serious damage to the permeability of the intestinal epithelium (Luo et al., 2019), which then impacts nutrient uptake (Lallès, 2019). Proteobacteria, Bacteroidetes, Firmicutes and Spirochaetes were the major bacterial phyla in jacopever intestines (Fig. 3, Table S1), which was consistent with the major bacterial phyla detected in the seawater (Sun et al., 2020a). Specific and shared operational taxonomic units, the mean relative abundance between groups and the top 10 most abundant species in all groups are shown in Fig. 3B and C. Differences in the relative abundance of bacteria were observed among control, PS-MPs and PS-NPs groups, indicating that the PS-NPs and PS-MPs can interfere with the composition of the intestinal microbial community. However, only specific bacterial genera in PS-NPs groups (*Brevundimona*) and PS-MPs group (*Tropicibacter*, *Nautella*, *Parasutterella* and *Thalassotalea*) were found to have significant differences relative to the control groups ($p < 0.05$) (Table S2), and there were no significant differences in Shannon index between the different groups (Fig. 3D). Kyoto Encyclopedia of Genes and Genomes (KEGG) database analysis associated with gut microbiota showed no significant differences were observed among all the groups ($P > 0.05$) (Fig. 3E, Table S3). Additionally, only the cell motility of the PS-MPs group was significant lower than that of the PS-NPs and control groups (Fig. 3F), demonstrating the intestinal bacteria were more like to attach onto PS-MPs rather than PS-NPs.

3.5. Liver transcriptomic response

RNA-seq was utilized to explore the target gene(s) for PS-MPs and PS-NPs disruption of liver metabolism homeostasis. Significant differential expression of genes (326, 253, and 66) was observed in control-vs-MP, control-vs-NP, and MP-vs-NP liver samples, with 278, 216 and 16 genes for up-regulation, and 48, 37 and 50 genes for down-regulation, respectively (Fig. S6A). There was a notable correlation ($r = 0.8901$) between q-PCR and RNA sequencing for the 28 selected genes involved

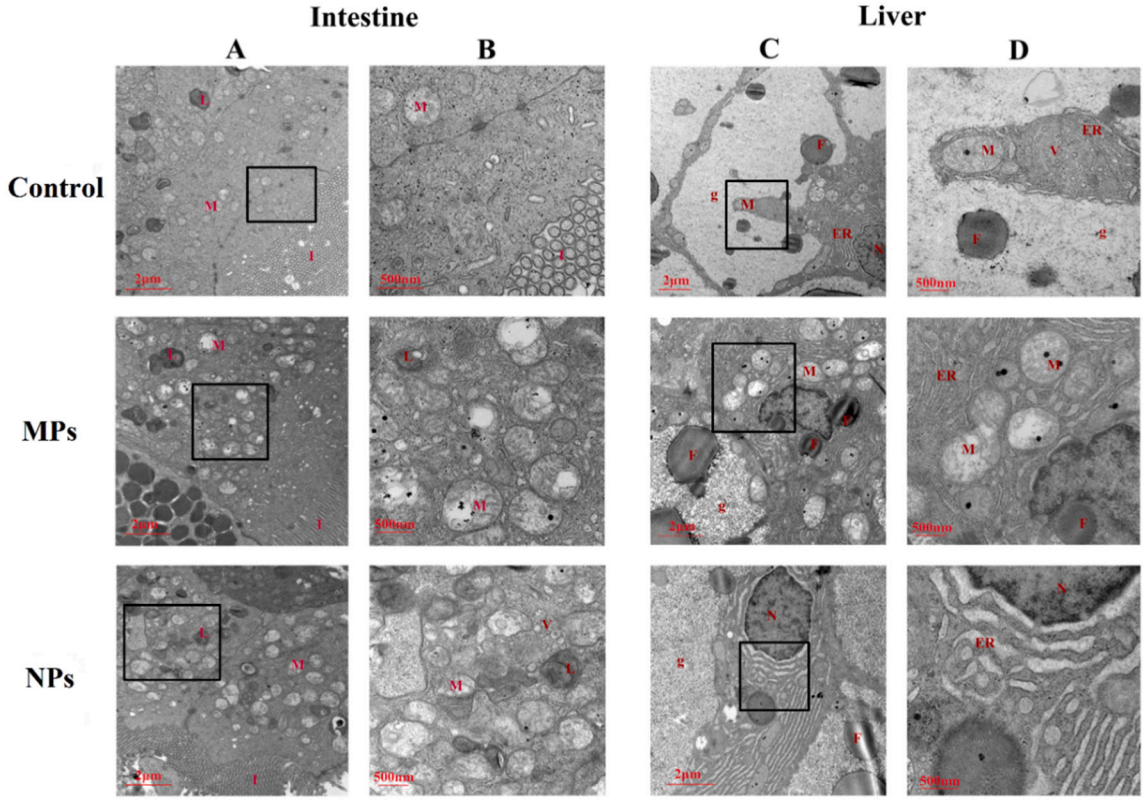

Fig. 2. Transmission electron microscope (TEM) images of *S. schlegelii* exposed to PS-NPs and PS-MPs. (A, B) intestine cells, (C, D) hepatic cells. (B) and (D) are magnified images of the areas outlined by the dotted rectangle in (A) and (C), respectively. Abbreviations: ER = endoplasmic reticulum, M = mitochondria, N = nucleus, V = vacuole, L = lysosome, F = fat droplet, I = intestinal villi, g = glycogen granules.

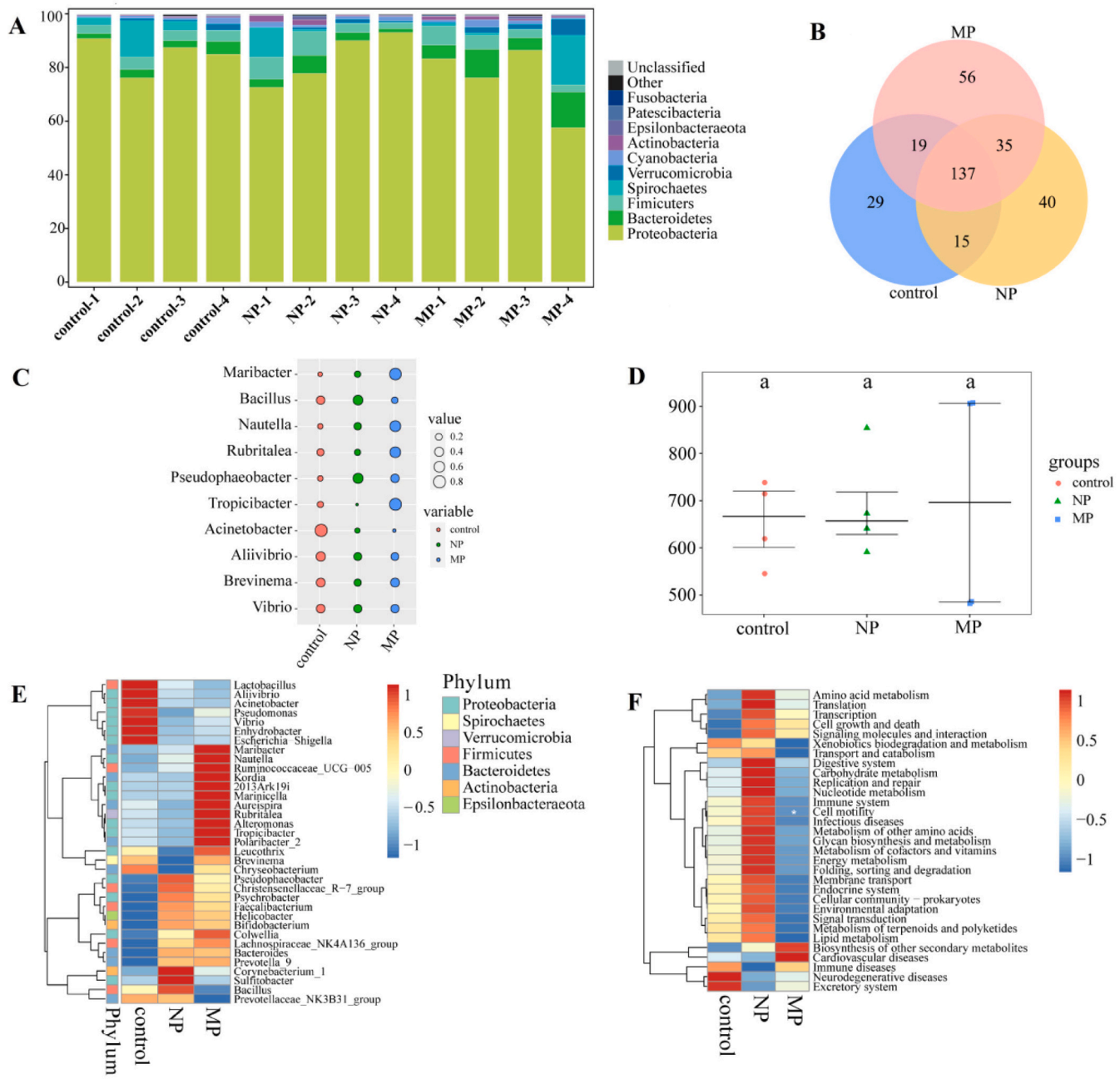

Fig. 3. Microbiome analysis of the intestine of *S. schlegelii* exposed to PS-MPs and PS-NPs for 15 days using 16S rDNA sequencing. (A) Microbiota composition at the phylum level, (B) Venn diagram showing specific and shared operational taxonomic units with the mean relative abundance between groups, (C) The top 10 most abundant species and the number of tags >2000 in all groups, (D) Alpha diversity (Shannon diversity), (E) Heatmap constructed with the top 35 most abundant genera, and (F) Heatmap of predicted functional categories. PICRUST was used to predict and compare the functions of bacterial microbiota using the KEGG database at level 2 ($n = 4$ per group).

in metabolism, immune system, and apoptosis, indicating that the expression trends of the DEGs identified by q-PCR were consistent with those detected by RNA-seq analysis (Fig. S6B, Table S4).

There were significant differences between the PS-MPs and PS-NPs groups in the membrane, vesicle, actin-based activity, and substance transport and metabolic based on cellular component category ($p < 0.05$), and transport activity, protein binding, ion binding, and actin binding based on molecular function category ($p < 0.05$) (Fig. 4A and S7). This appears to be associated with the cellular internalization (Roth, 2007) and indicates a significantly different level of endocytosis for PS-MPs and PS-NPs. The endocytosis was influenced by particle size, surface charge and surface composition, which affected their internalization pathways (Alimba et al., 2021; Liu et al., 2021). Nano-sized particles might interact with small biomolecules (e.g., amino acids, sugars and ions) and traverse the plasma membrane through the action of (i) integral membrane protein pumps or channels, and (ii) clathrin/caveolin-mediated endocytosis (Chakravarty et al., 2010; Prakash et al., 2021). Accordingly, the upregulation of amino acid transporter (*SLC15A1*), solution carrier family member (*SLC43A2*, *SLC25A48*, *SLC15A1*), and transmembrane protein (*TM4SF1*) genes appeared as a stress response to PS-NPs exposure (Fig. S8). In contrast, the large sized PS-MPs might be transported into the cell by phagocytosis or pinocytosis, such as membrane bound vesicles in a process termed micropinocytosis (Conner and Schmid, 2003; Liu et al., 2021). Accordingly,

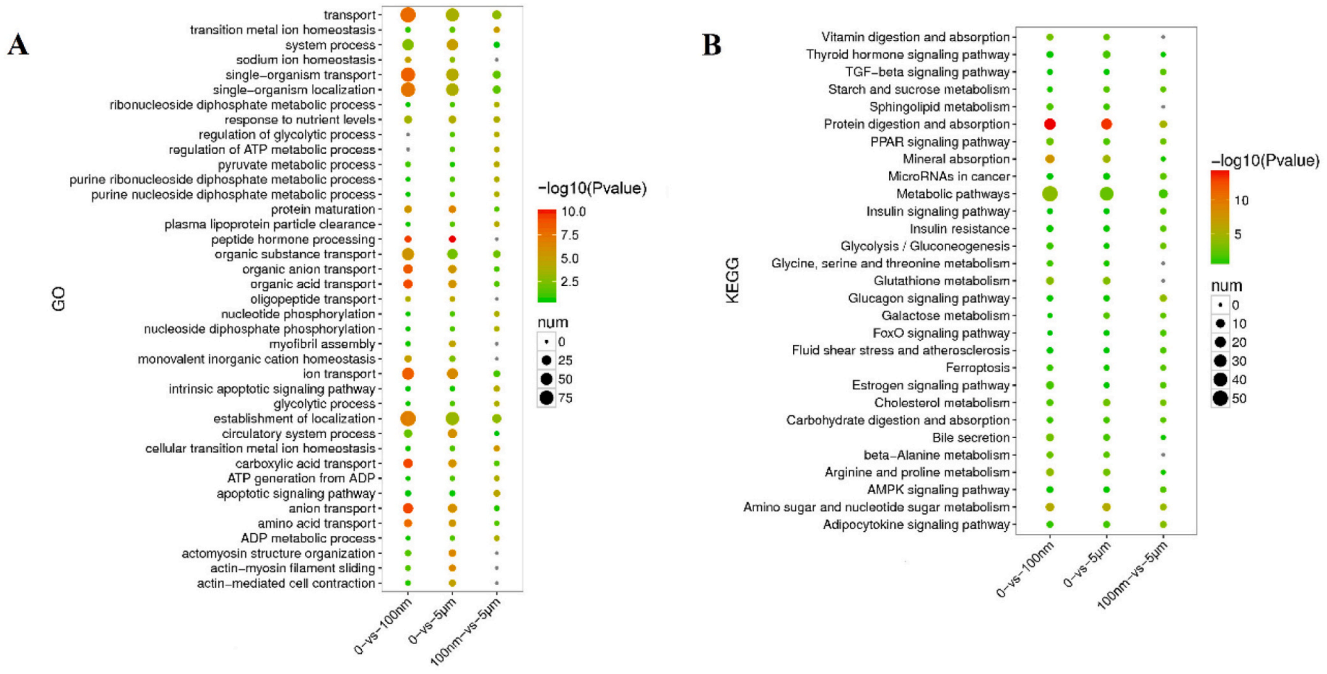

Fig. 4. Transcriptome analysis of *S. schlegelii* exposed to PS-MPs and PS-NPs. (A) The top 20 GO terms (biological process) with significant enrichment of DEGs in the liver exposed to PS-MPs and PS-NPs ($p < 0.05$). (B) The top 20 KEGG pathways with significant enrichment of DEGs in the visceral mass exposed to MPs and NPs ($p < 0.05$).

the upregulation of vacuolar protein (*VPS26C*), actin (*ACT2*), myosin (*MYH*) and tubulin (*TUBB2B*) genes was found in the PS-MPs groups (Fig. S8B). A previous study reported that the endocytosis of 50 nm PS-NPs occurred through a combination of the clathrin-mediated pathway, the caveolin-mediated pathways and macropinocytosis, while endocytosis of 500 nm PS-NPs was mainly via micropinocytosis (Liu et al., 2021).

KEGG analysis identified 19 significantly different pathways between the PS-NPs and PS-MPs groups ($p < 0.05$) (Fig. 4B). These pathways were concentrated in (i) protein, vitamin and carbohydrate digestion and absorption, (ii) sugar, amino and lipid metabolism, and the (iii) signal pathways related to oxidative stress and immune response (Table S5). Oxidative damage was another important impact induced by PS-MPs/NPs, which can lead to genomic instability (Kim et al., 2021). Several differentially expressed genes (DEGs; *CYP4B1*, *CYP2K1*, *CYP27C1*) related to oxidative stress were significantly overexpressed in the PS-NPs and PS-MPs groups compared with control groups. To explore oxidative damage of liver after exposure to PS-MPs/PS-NPs, the malondialdehyde (MDA) content and antioxidative enzyme (SOD and CAT) activities of liver were investigated (Fig. S9). The results showed the stronger oxidative stress and lipid peroxidation induced by the PS-NPs than the PS-MPs. Similarly, oxidative stress-triggered mitochondrial depolarization, suppression of fatty acid oxidation and transport, and promotion of inflammation were identified as the key mechanisms for the hepatotoxicity of photodegraded PS-MPs to grouper (Wang et al., 2020). In addition to the DEGs related to oxidative stress, a large number of DEGs also existed in the substance and energy metabolism, cell process and signal transduction categories (Fig. S8). The bacteria abundance has no significant correlation with the gene expression and antioxidative enzyme activities (Fig. S10).

3.6. Liver metabolomic alterations

When compared to PS-NPs groups, the MPs groups displayed significant variation ($p < 0.05$) in 345 metabolites (Fig. S11). The top 250 most significantly different metabolites and genes were used to construct an integrated network of functional interactions between the PS-MPs and the PS-NPs, which showed >80 % of gene expressions were negatively related to the metabolites (Fig. 5F). Importantly, the increase of genes related to liver metabolism in the PS-NPs group were highly consistent with the decrease in metabolites synthesis related to amino acid, carbohydrate, nucleoside alkaloids, fatty acid and glycerol phospholipid metabolism (Fig. 5A–E). These metabolites contained human-essential amino acids (e.g., isoleucine, racemethionine, threonine, valine, phenylalanine and lysine), omega-3 fatty acids (e.g., docosahexaenoic acid, eicosapentaenoic acid), an intermediate product of glucose metabolism (e.g., gluconic acid) and tricarboxylic acid (TCA) cycle metabolites (e.g., malic acid and cis-aconitate), as well as other compounds associated with nutritional quality. However, only one human-essential amino acid and one omega-3 fatty acid were significantly decreased in the PS-MPs groups relative to those in the control groups ($p < 0.05$).

The KEGG pathways analysis of liver metabolomic alterations showed that more significant changes appeared in the PS-NPs groups compared with the PS-MPs groups ($p < 0.05$). These were not only concentrated in the lipid metabolism, but also in the TCA cycle, ABC transporters, protein digestion and absorption, and cell apoptosis (Ferroptosis and FoxO signaling pathways) (Table S5), which was in accordance with results of the transcriptome KEGG pathways analysis. However, bile secretion, as well as taurine and hypotaurine metabolism, was enhanced in the PS-MPs but not in the PS-NPs groups. Previous studies have also found that MPs can induce disruption of bile acid metabolism in animals (Yin et al., 2018; Zhang et al., 2022), influence combination of bile acids and taurine involved the enterohepatic circulation, and regulate lipid and glucose metabolism (Martins et al., 2021; Seymour and Geyer, 1992). The results of this study indicate that PS-NPs and PS-MPs can differently impact the metabolic homeostasis of fish livers and DEGs in a range of KEGG pathways (Fig. S11). Overall, impacts mainly followed the order of PS-NPs > PS-MPs > control. These results explain the quantifiable reduction in nutritional quality observed for *S. schlegelii* in the PS-NPs groups relative to the PS-MPs group (Table 1).

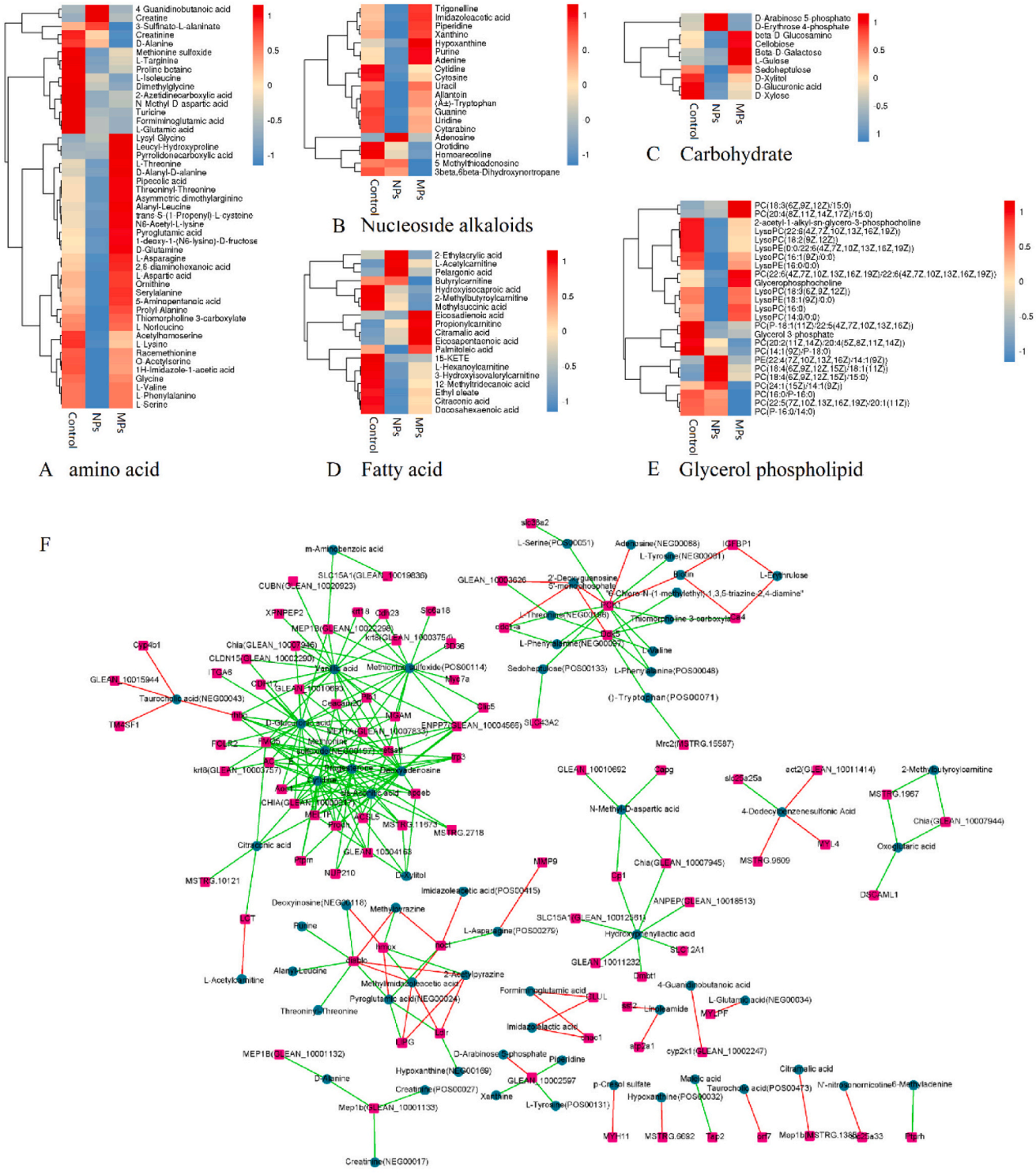

Fig. 5. The significantly different metabolites associated with the key pathways affected by PS-MPs and PS-NPs exposure in *S. schlegelii*. (A) amino acid, (B) Nucleoside alkaloids, (C) Carbohydrate, (D) Fatty acid, (E) Glycerol phospholipid, and (F) Integrated network of functional interactions between metabolites (represented by their index-codes) and genes (represented by their ZFIN official names) whose levels were affected in fish liver by PS-MPs and PS-NPs exposure. The metabolites and genes were indicated by blue and pink, respectively. Red and blue lines represent positive and negative correlation, respectively.

Mitochondria, the main target organelle for nanomaterials, plays a critical role in their toxic activities (Nichols et al., 2018; Yang et al., 2016). The histopathological and ultrastructural alterations showed both PS-NPs and PS-MPs could induce mitochondrial disruption of hepatocytes (Fig. 2D and F). Meanwhile, a significant upregulation of *PRODH* and *SLC25A25A* was detected in the PS-NPs groups relative to the PS-MPs and control groups (Fig. S8), which is associated with the electron transfer chain and protects against oxidative damage of the mitochondria (Hirschenson and Mailloux, 2021; Moreira et al., 2019). Similarly, a significantly different metabolic pathway of ubiquinone (UQ) and other terpenoid-quinone biosynthesis was observed for PS-NPs (Table S6), which is associated with regulation of ATP generation of

mitochondria through controlling calcium homeostasis (Anunciado-Koza et al., 2011; Hao et al., 2018). The damage of mitochondria will influence the TCA cycle (Chen et al., 2022; Martinez-Reyes and Chandel, 2020). The TCA cycle metabolites (cis-aconitate and malic acid) were significantly reduced in the PS-NPs group compared with control group, while only the cis-aconitate was significantly reduced in the PS-MPs group compared with control group (Fig. S8). PS-NPs uptake into the hepatocyte mainly occurred through membrane protein pumps or channels, and clathrin/caveolin-mediated endocytosis, while PS-MPs were taken up through phagocytosis or pinocytosis, which triggered different energy and material metabolism. Furthermore, the PS-NPs induced a more serious oxidative stress and lipid peroxidation response than PS-MPs, and with the help of signal transduction, additionally destroyed the structural integrity of mitochondria and triggered cell apoptosis, decreasing the overall nutritional quality of fish (Fig. 6).

4. Conclusions

Overall, the effects of PS-MPs and PS-NPs on the nutritional quality of marine fish and the underlying mechanisms of toxicity were successfully elucidated. Although the sedimentation rate of PS-MPs in seawater was lower than that of PS-NPs at the same concentration (by mass), the PS-NPs had a greater effect than the PS-MPs on the energy reserve and nutritional quality of marine jacopever. At environmentally relevant concentrations, neither PS-NPs nor PS-MPs had a significant impact on the intestinal microbiota composition. However, they cause different pathological changes in the epithelial cells of intestine, and in hepatocytes of liver. Uptake of PS-NPs and PS-MPs by hepatocytes

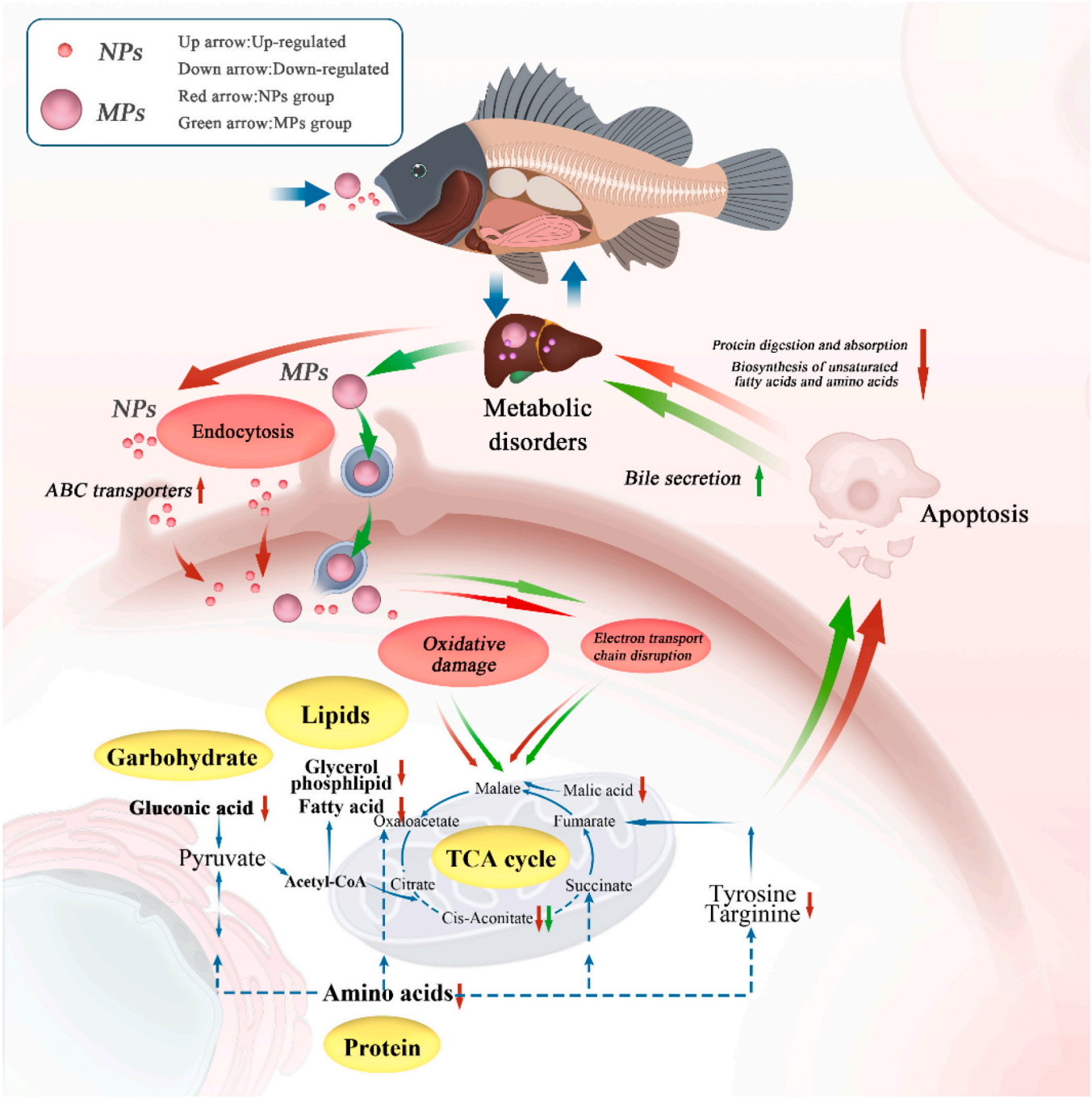

Fig. 6. Schematic illustration of the toxicity mechanisms for PS-MPs and PS-NPs in the liver of *S. schlegelii*.

mainly occurred through different forms of endocytosis, which triggered different cell signal transduction, including an apoptosis signal for hepatocytes. Importantly, the uptake of PS-NPs by hepatocytes induced more serious oxidative damage than PS-MPs, as well as destroying the structural integrity of mitochondria and influencing the release of TCA cycle metabolites. Therefore, PS-NP exposure can cause more greater decrease in the economic benefits of mariculture and the supply of high-quality protein for human beings than PS-MPs. Considering that secondary NPs are thought to be more prevalent than primary NPs and MPs, further studies should be performed to (i) determine the NP concentrations in the marine environment, (ii) study the toxicological impacts of a broader range of polymer types, and (iii) assess the effects of environmental relevant NPs (e.g., secondary NPs).

CRediT authorship contribution statement

Xuemei Sun: Methodology, Investigation, Writing - original draft. **Bin Xia and Andy M. Booth**: Conceived the framework, Writing - review & editing, Funding acquisition. **Xuru Wang**: Methodology, Investigation; **Lin Zhu and Qi Sui**: Formal analysis, Writing - review & editing; **Bijuan Chen and Keming Qu**: Supervision.

Declaration of competing interest

The authors declare that they have no known competing financial interests or personal relationships that could have appeared to influence the work reported in this paper.

Data availability

The data that has been used is confidential.

Acknowledgement

This project is supported by the NSFC-Shandong Joint Fund for Marine Ecology and Environmental Sciences (U2106213), National Natural Science Foundation of China (42107137, 41976143), Laoshan Laboratory (LSKJ202203903), the National Key Research and Development Program of China (2018YFD0900703), the Key Technology Research and Development Program of Shandong Province (2022CXPT013), Taishan Scholars Program of Shandong Province (tsqn202211267), and Central Public-interest Scientific Institution Basal Research Fund, CAFS (2020TD12).

Appendix A. Supplementary data

Additional details on MPs and NPs characterization and size distribution determination, culture and exposure experiment conditions, oxidative stress, histological and intestinal microbiota analysis, DNA and RNA Extraction and q-PCR; 11 figures; 6 tables, and additional references 3. Supplementary data to this article can be found online at doi:https://doi.org/10.1016/j.scitotenv.2023.166560.

References

Alimba, C.G., Faggio, C., Sivanesan, S., Ogunkanmi, A.L., Krishnamurthi, K., 2021. Micro (nano)-plastics in the environment and risk of carcinogenesis: insight into possible mechanisms. J. Hazard. Mater. 416, 126143.

Anunciado-Koza, R.P., Zhang, J., Ukropec, J., Bajpeyi, S., Koza, R.A., Rogers, R.C., Cefalu, W.T., Mynatt, R.L., Kozak, L.P., 2011. Inactivation of the mitochondrial carrier *SLC25A25* (ATP-Mg^{2+}/pi transporter) reduces physical endurance and metabolic efficiency in mice. J. Biol. Chem. 286 (13), 11659–11671.

Awad, W.A., Ruhnau, D., Hess, C., Doupovec, B., Schatzmayr, D., Hess, M., 2019. Feeding of deoxynivalenol increases the intestinal paracellular permeability of broiler chickens. Arch. Toxicol. 93 (7), 2057–2064.

Booth, A.M., Justynska, J., Kubowicz, S., Johnsen, H., Frenzel, M., 2013. Influence of salinity, dissolved organic carbon and particle chemistry on the aggregation behaviour of methacrylate-based polymeric nanoparticles in aqueous environments. Int. J. Environ. Pollut. 52 (1/2), 15–31.

Chakravarty, P., Qian, W., El-Sayed, M.A., Prausnitz, M.R., 2010. Delivery of molecules into cells using carbon nanoparticles activated by femtosecond laser pulses. Nat. Nanotechnol. 5 (8), 607–611.

Chen, Y., Li, J., Yuan, P., Wu, Z., Wang, Z., Wu, W., 2022. Graphene oxide promoted chromium uptake by zebrafish embryos with multiple effects: adsorption, bioenergetic flux and metabolism. Sci. Total Environ. 802, 149914.

Conner, S.D., Schmid, S.L., 2003. Regulated portals of entry into the cell. Nature 422 (6927), 37–44.

Davranche, M., Lory, C., Juge, C.L., Blancho, F., Dia, A., Grassl, B., El Hadri, H., Pascal, P.-Y., Gigault, J., 2020. Nanoplastics on the coast exposed to the North Atlantic Gyre: evidence and traceability. NanoImpact 20, 100262.

Duan, Z., Cheng, H., Duan, X., Zhang, H., Wang, Y., Gong, Z., Zhang, H., Sun, H., Wang, L., 2022. Diet preference of zebrafish (*Danio rerio*) for bio-based polylactic acid microplastics and induced intestinal damage and microbiota dysbiosis. J. Hazard. Mater. 429, 128332.

Duparc, T., Plovier, H., Marrachelli, V.G., Van Hul, M., Essaghir, A., Stahlman, M., Matamoros, S., Geurts, L., Pardo-Tendero, M.M., Druart, C., Delzenne, N.M., Demoulin, J.B., van der Merwe, S.W., van Pelt, J., Backhed, F., Monleon, D., Everard, A., Cani, P.D., 2017. Hepatocyte MyD88 affects bile acids, gut microbiota and metabolome contributing to regulate glucose and lipid metabolism. Gut 66 (4), 620–632.

Gaylarde, C.C., Baptista Neto, J.A., da Fonseca, E.M., 2021. Nanoplastics in aquatic systems - are they more hazardous than microplastics? Environ. Pollut. 272, 115950.

Gopinath, P.M., Saranya, V., Vijayakumar, S., Mythili Meera, M., Ruprekha, S., Kunal, R., Pranay, A., Thomas, J., Mukherjee, A., Chandrasekaran, N., 2019. Assessment on interactive prospectives of nanoplastics with plasma proteins and the toxicological impacts of virgin, coronated and environmentally released-nanoplastics. Sci. Rep. 9 (1), 8860.

Grisdale-Helland, B., Shearer, K.D., Gatlin, D.M., Helland, S.J., 2008. Effects of dietary protein and lipid levels on growth, protein digestibility, feed utilization and body composition of Atlantic cod (*Gadus morhua*). Aquaculture 283 (1–4), 156–162.

Hamed, M., Monteiro, C.E., Sayed, A.E.H., 2022. Investigation of the impact caused by different sizes of polyethylene plastics (nano, micro, and macro) in common carp juveniles, *Cyprinus carpio* L., using multi-biomarkers. Sci. Total Environ. 803, 149921.

Hao, L., Sun, Q., Zhong, W., Zhang, W., Sun, X., Zhou, Z., 2018. Mitochondria-targeted ubiquinone (MitoQ) enhances acetaldehyde clearance by reversing alcohol-induced posttranslational modification of aldehyde dehydrogenase 2: a molecular mechanism of protection against alcoholic liver disease. Redox Biol. 14, 626–636.

Hirschenson, J., Mailloux, R.J., 2021. The glutathionylation agent disulfiram augments superoxide/hydrogen peroxide production when liver mitochondria are oxidizing ubiquinone pool-linked and branched chain amino acid substrates. Free Radic. Biol. Med. 172, 1–8.

Jeong, C.B., Won, E.J., Kang, H.M., Lee, M.C., Hwang, D.S., Hwang, U.K., Zhou, B., Souissi, S., Lee, S.J., Lee, J.S., 2016. Microplastic size-dependent toxicity, oxidative stress induction, and p-JNK and p-p38 activation in the Monogonont Rotifer (*Brachionus koreanus*). Environ. Sci. Technol. 50 (16), 8849–8857.

Kim, J.H., Yu, Y.B., Choi, J.H., 2021. Toxic effects on bioaccumulation, hematological parameters, oxidative stress, immune responses and neurotoxicity in fish exposed to microplastics: a review. J. Hazard. Mater. 413, 125423.

Kishimura, H., Tokuda, Y., Yabe, M., Klomklao, S., Benjakul, S., Ando, S., 2007. Trypsins from the pyloric ceca of jacopever (*Sebastes schlegelii*) and Elkhorn sculpin (*Alcichthys alcicornis*): isolation and characterization. Food Chem. 100 (4), 1490–1495.

Lai, W., Xu, D., Li, J., Wang, Z., Ding, Y., Wang, X., Li, X., Xu, N., Mai, K., Ai, Q., 2021. Dietary polystyrene nanoplastics exposure alters liver lipid metabolism and muscle nutritional quality in carnivorous marine fish large yellow croaker (*Larimichthys crocea*). J. Hazard. Mater. 419, 126454.

Lallès, J.P., 2019. Intestinal alkaline phosphatase in the gastrointestinal tract of fish: biology, ontogeny, and environmental and nutritional modulation. Rev. Aquac. 12 (2), 555–581.

Lee, C.H., Fang, J.K., 2022. Effects of temperature and particle concentration on aggregation of nanoplastics in freshwater and seawater. Sci. Total Environ. 817, 152562.

Lenz, R., Enders, K., Nielsen, T.G., 2016. Microplastic exposure studies should be environmentally realistic. Proc. Natl. Acad. Sci. 113 (29), E4121–E4122.

Li, X., He, E., Jiang, K., Peijnenburg, W., Qiu, H., 2021a. The crucial role of a protein corona in determining the aggregation kinetics and colloidal stability of polystyrene nanoplastics. Water Res. 190, 116742.

Li, B., Liang, W., Liu, Q.X., Fu, S., Ma, C., Chen, Q., Su, L., Craig, N.J., Shi, H., 2021b. Fish ingest microplastics unintentionally. Environ. Sci. Technol. 55 (15), 10471–10479.

Liu, J., Legros, S., Ma, G., Veinot, J.G., von der Kammer, F., Hofmann, T., 2012. Influence of surface functionalization and particle size on the aggregation kinetics of engineered nanoparticles. Chemosphere 87 (8), 918–924.

Liu, L., Xu, K., Zhang, B., Ye, Y., Zhang, Q., Jiang, W., 2021. Cellular internalization and release of polystyrene microplastics and nanoplastics. Sci. Total Environ. 779, 146523.

Lu, X., Deng, D.F., Huang, F., Casu, F., Kraco, E., Newton, R.J., Zohn, M., Teh, S.J., Watson, A.M., Shepherd, B., Ma, Y., Dawood, M.A.O., Rios Mendoza, L.M., 2022. Chronic exposure to high-density polyethylene microplastic through feeding alters the nutrient metabolism of juvenile yellow perch (*Perca flavescens*). Anim. Nutr. 9, 143–158.

Luo, T., Wang, C., Pan, Z., Jin, C., Fu, Z., Jin, Y., 2019. Maternal polystyrene microplastic exposure during gestation and lactation altered metabolic homeostasis in the dams and their F1 and F2 offspring. Environ. Sci. Technol. 53 (18), 10978–10992.

Ma, C., Chen, Q., Li, J., Li, B., Liang, W., Su, L., Shi, H., 2022. Distribution and translocation of micro- and nanoplastics in fish. Crit. Rev. Toxicol. 1–14.

Magalhaes, J.G., Tattoli, I., Girardin, S.E., 2007. The intestinal epithelial barrier: how to distinguish between the microbial flora and pathogens. Semin. Immunol. 19 (2), 106–115.
Magri, D., Sanchez-Moreno, P., Caputo, G., Gatto, F., Veronesi, M., Bardi, G., Catelani, T., Guarnieri, D., Athanassiou, A., Pompa, P.P., Fragouli, D., 2018. Laser ablation as a versatile tool to mimic polyethylene terephthalate nanoplastic pollutants: characterization and toxicology assessment. ACS Nano 12 (8), 7690–7700.
Martinez-Negro, M., Gonzalez-Rubio, G., Aicart, E., Landfester, K., Guerrero-Martinez, A., Junquera, E., 2021. Insights into colloidal nanoparticle-protein corona interactions for nanomedicine applications. Adv. Colloid Interf. Sci. 289, 102366.
Martinez-Reyes, I., Chandel, N.S., 2020. Mitochondrial TCA cycle metabolites control physiology and disease. Nat. Commun. 11 (1), 102.
Martins, N., Diógenes, A.F., Magalhães, R., Matas, I., Oliva-Teles, A., Peres, H., 2021. Dietary taurine supplementation affects lipid metabolism and improves the oxidative status of European seabass (*Dicentrarchus labrax*) juveniles. Aquaculture 531, 735820.
Moreira, J.B.N., Wohlwend, M., Fenk, S., Amellem, I., Flatberg, A., Kraljevic, J., Marinovic, J., Ljubkovic, M., Bjorkoy, G., Wisloff, U., 2019. Exercise reveals proline dehydrogenase as a potential target in heart failure. Prog. Cardiovasc. Dis. 62 (2), 193–202.
Nguyen, P., Leray, V., Diez, M., Serisier, S., Le Bloc'h, J., Siliart, B., Dumon, H., 2008. Liver lipid metabolism. J. Anim. Physiol. Anim. Nutr. 92 (3), 272–283.
Nichols, C.E., Shepherd, D.L., Hathaway, Q.A., Durr, A.J., Thapa, D., Abukabda, A., Yi, J., Nurkiewicz, T.R., Hollander, J.M., 2018. Reactive oxygen species damage drives cardiac and mitochondrial dysfunction following acute nano-titanium dioxide inhalation exposure. Nanotoxicology 12 (1), 32–48.
Prakash, S., Kumbhojkar, N., Clegg, J.R., Mitragotri, S., 2021. Cell-bound nanoparticles for tissue targeting and immunotherapy: engineering of the particle-membrane interface. Curr. Opin. Colloid Interface Sci. 52, 101408.
Rocha, T.L., Gomes, T., Sousa, V.S., Mestre, N.C., Bebianno, M.J., 2015. Ecotoxicological impact of engineered nanomaterials in bivalve molluscs: an overview. Mar. Environ. Res. 111, 74–88.
Roth, M.G., 2007. Integrating actin assembly and endocytosis. Dev. Cell 13 (1), 3–4.
Seymour, R.J., Geyer, R.A., 1992. Fates and effects of oil spills. Annu. Rev. Env. 17, 261–283.
Sun, X., Chen, B., Xia, B., Li, Q., Zhu, L., Zhao, X., Gao, Y., Qu, K., 2020a. Impact of mariculture-derived microplastics on bacterial biofilm formation and their potential threat to mariculture: a case in situ study on the Sungo Bay, China. Environ. Pollut. 262, 114336.
Sun, X.D., Yuan, X.Z., Jia, Y., Feng, L.J., Zhu, F.P., Dong, S.S., Liu, J., Kong, X., Tian, H., Duan, J.L., Ding, Z., Wang, S.G., Xing, B., 2020b. Differentially charged nanoplastics demonstrate distinct accumulation in *Arabidopsis thaliana*. Nat. Nanotechnol. 15 (9), 755–760.
Ter Halle, A., Jeanneau, L., Martignac, M., Jarde, E., Pedrono, B., Brach, L., Gigault, J., 2017. Nanoplastic in the North Atlantic Subtropical Gyre. Environ. Sci. Technol. 51 (23), 13689–13697.
Wagner, S., Reemtsma, T., 2019. Things we know and don't know about nanoplastic in the environment. Nat. Nanotechnol. 14 (4), 300–301.
Wang, X., Zheng, H., Zhao, J., Luo, X., Wang, Z., Xing, B., 2020. Photodegradation elevated the toxicity of polystyrene microplastics to grouper (*Epinephelus moara*) through disrupting hepatic lipid homeostasis. Environ. Sci. Technol. 54 (10), 6202–6212.
Wang, Z., Yin, L., Zhao, J., Xing, B., 2016. Trophic transfer and accumulation of TiO_2 nanoparticles from clamworm (*Perinereis aibuhitensis*) to juvenile turbot (*Scophthalmus maximus*) along a marine benthic food chain. Water Res. 95, 250–259.
Wu, C., Guo, W.B., Liu, Y.Y., Yang, L., Miao, A.J., 2021. Perturbation of calcium homeostasis and multixenobiotic resistance by nanoplastics in the ciliate *Tetrahymena thermophila*. J. Hazard. Mater. 403, 123923.
Xia, B., Zhang, J., Zhao, X., Feng, J., Teng, Y., Chen, B., Sun, X., Zhu, L., Sun, X., Qu, K., 2020. Polystyrene microplastics increase uptake, elimination and cytotoxicity of decabromodiphenyl ether (BDE-209) in the marine scallop *Chlamys farreri*. Environ. Pollut. 258, 113657.
Yang, L.Y., Gao, J.L., Gao, T., Dong, P., Ma, L., Jiang, F.L., Liu, Y., 2016. Toxicity of polyhydroxylated fullerene to mitochondria. J. Hazard. Mater. 301, 119–126.
Yin, L., Chen, B., Xia, B., Shi, X., Qu, K., 2018. Polystyrene microplastics alter the behavior, energy reserve and nutritional composition of marine jacopever (*Sebastes schlegelii*). J. Hazard. Mater. 360, 97–105.
Zhang, C., Jeong, C.B., Lee, J.S., Wang, D., Wang, M., 2019. Transgenerational proteome plasticity in resilience of a marine copepod in response to environmentally relevant concentrations of microplastics. Environ. Sci. Technol. 53 (14), 8426–8436.
Zhang, X., Zhou, Q., Zou, W., Hu, X., 2017. Molecular mechanisms of developmental toxicity induced by graphene oxide at predicted environmental concentrations. Environ. Sci. Technol. 51 (14), 7861–7871.
Zhang, X., Wen, K., Ding, D., Liu, J., Lei, Z., Chen, X., Ye, G., Zhang, J., Shen, H., Yan, C., Dong, S., Huang, Q., Lin, Y., 2021b. Size-dependent adverse effects of microplastics on intestinal microbiota and metabolic homeostasis in the marine medaka (*Oryzias melastigma*). Environ. Int. 151, 106452.
Zhang, X., Xia, M., Zhao, J., Cao, Z., Zou, W., Zhou, Q., 2022. Photoaging enhanced the adverse effects of polyamide microplastics on the growth, intestinal health, and lipid absorption in developing zebrafish. Environ. Int. 158, 106922.
Zhang, Z.H., Fu, Y.Q., Guo, H.Y., Zhang, X.M., 2021a. Effect of Environmental Enrichment on the Stress Response of Juvenile Black Rockfish *Sebastes schlegelii*, 533, p. 736088.
Zhu, L., Qu, K., Xia, B., Sun, X., Chen, B., 2016. Transcriptomic response to water accommodated fraction of crude oil exposure in the gill of Japanese flounder, *Paralichthys olivaceus*. Mar. Pollut. Bull. 106 (1–2), 283–291.